Electronic Supplementary Material (ESI) for Journal of Materials Chemistry A.

Supplemental Information

Post-Synthesis of Covalent Organic Frameworks Nanofiltration Membrane for Highly Efficient Water Treatment

Chuanyao Liu [a], Yunzhe Jiang [a], Anjaiah Nalaparaju [b], Jianwen Jiang [b]*, and Aisheng Huang [a]*

[a] Shanghai Key Laboratory of Green Chemistry and Chemical Processes, Department of Chemistry, East China Normal University, Dongchuan Road 500, Shanghai 200241, China

[b] Department of Chemical and Biomolecular Engineering, National University of Singapore, 117576, Singapore

* Corresponding author. Tel.: +86-21-33503037; Fax: +86-21-33503037.
E-mail address: huangash@chem.ecnu.edu.cn

Experimental details:

Chemicals: Chemicals were used as received without further purification. 3,5-diamino-1,2,4-triazole (Aladdin, 98%), hexamethylenetetramine (Energy chemical, 97%) and m-trihydroxybenzene(Energy chemical，99%), Trifluroacetic acid (CF_3COOH, Energy chemical，99%), chloroform (Sinopharm, 99%), (3-aminopropyl)triethoxysilane (APTES, Aladdin, 99%), Succinic anhydride (SA, Aladdin, 99%)，dioxane (Greagent, 99.5%), dimethylacetamide (DMAc, Aladdin, 99.5%), hydrochloric Acid (HCl, Sinopharm, AR), acetic acid (HAc, Sinopharm, AR), ethanol (anhydrous, Greagent, > 99.7%), HCl (Sinopharm, 37%), toluene (99%, Aladdin), acetone (99.5%, Aladdin); NaCl (Aladdin, 99%), Na_2SO_4 (Aladdin, 99%)，$FeCl_3$ (Aladdin, 99%)， $MgCl_2$ (Aladdin, 99%)，and $MgSO_4$ (Aladdin, 99%)，deionized water (home-made). Porous α-Al_2O_3 tubes (Jiexi Lishun Technology Co., Guangdong, China: 12 mm outside diameter, 9 mm inside diameter, 75 mm length, ca. 1.0 μm pore size, 30% porosity) were used as the supports.

Synthesis of 1,3,5-tris(4-formylphenyl)benzene (TFP): 1,3,5-tris(4-formylphenyl)benzene (TFP) was synthesized according to a reported procedure with slight modification. [1] Under a nitrogen atmosphere, hexamethylenetetramine (15.098 g, 108 mmol) and m-trihydroxybenzene (6.014 g, 49 mmol) were added to a solution of 90 mL CF_3COOH in a 500 mL three-necked bottle at 25 °C. The mixture was heated at 70 ^oC and stirred for 1.5 hours. Then 150 mL of 3 M HCl was added to the reaction solution and reacted for another 2 hours. After cooling to room temperature, the reaction mixture was filtered and extracted with ca. 200 mL dichloromethane. The filtrate was concentrated on a rotary evaporator. The crude residue was purified by washing with hot ethanol to give pure TFP as a yellow solid, 1.24 g (12% yield). 1H NMR (400 MHz, $CDCl_3$): δ 14.12 (s, 3H, OH), 10.16 (s, 3H, CHO) ppm.

Synthesis of IISERP-COF1 powders: IISERP-COF1 powders were synthesized mainly according to previous work [2] with minor modification. 1,3,5-tris(4-formylphenyl)benzene (90 mg, 0.42 mmol) was first dissolved in the dimethylacetamide (5 mL), follow by adding dioxane (55 mL) and 3,5-diamino-

1,2,4-triazole (45 mg, 0.45 mmol). After the light yellow color solution was formed, 5.0 mL of 6 M aqueous acetic acid was added. Then the resulting solution (COF mother solution) was introduced in a Teflon-lined autoclave (80 mL) and heated at 120 °C for 3 days. The resulting COF powders were subsequently washed with dioxane, MeOH, acetone and THF several times and dried in air at room temperature.

Synthesis of IISERP-COF1 membranes: Typically, the IISERP-COF1 membrane was prepared on the APTES-modified α-Al2O3 support. Porousα-Al2O3 tubes were treated with APTES (0.6 mM in 30 mL toluene) at 110 ^{o}C for 1.5 h, leading to the formation APTES monolayer on the surface of α-Al2O3 tubes. [3-7]

The APTES-modified α-Al2O3 tubes were first seeded with IISERP-COF1 crystals by *in situ* solvothermal synthesis in the mother solution containing 1,3,5-tris(4-formylphenyl)benzene (45 mg, 0.21 mmol), 3,5-diamino-1,2,4-triazole (22.5 mg, 22.5 mmol), dimethylacetamide (5 mL), dioxane (55 mL) and of 5.0 mL 6 M aqueous acetic acid. The crystallization was conducted at 120 °C for 1 day in a Teflon-lined stainless steel autoclave. After cooling to room temperature, the seeded α-Al_2O_3 tubes were intensively washed with dioxane, MeOH, acetone and THF several times, and then dried at room temperature. The crystals within the membrane layer were further fused together to form a continuous and well-intergrown polycrystalline IISERP-COF1 membrane by secondary growth in another COF mother solution which contains 1,3,5-tris(4-formylphenyl)benzene (90 mg, 0.42 mmol), dimethylacetamide (5 mL), dioxane (55 mL), 3,5-diamino-1,2,4-triazole (45 mg, 45 mmol) and 5.0 mL of 6 M aqueous acetic acid. The synthesis was conducted at 120 °C for 3 days. After cooling down to the room temperature, the α-Al_2O_3 tube supported IISERP-COF1 membrane was washed with dioxane, MeOH, acetone and THF several times, and then dried at 120 °C overnight.

Post-synthesis of IISERP-COOH-COF1 powders and membranes: For post-synthesis of IISERP-COOH-COF1 powders, IISERP-COF1 powders (38 mg, 0.1 mmol) were added into 8.0 mL SA

(1.0 M solution in anhydrous acetone). The reaction mixture was heated at 60 °C for 24 h. The precipitate was collected by centrifugation, and washed with anhydrous acetone three times. The powder was dried at 80 °C under vacuum overnight to give the IISERP-COOH-COF1. [8-9] As for post-synthesis of IISERP-COOH-COF1 membrane, the activated IISERP-COF1 membrane was put into a 40 mL glass vial, where was fill with 35 mL SA (1.0 M solution in anhydrous acetone). The reaction mixture was heated at 60 °C for 24 h. Thereafter, the post-synthesis functionalized COF membrane was taken out and washed with fresh 35 ml acetone for several days (by changing acetone solution every day).

Characterization

Characterization of IISERP-COOH-COF1 powder and membrane: Micro-morphologies and elemental analysis of the membranes were performed on a field emission scanning electron microscopy (FESEM). FESEM micrographs were taken on an S-4800 (Hitachi) with a cold field emission gun operating at 4 kV and 10 μA. Energy dispersive X-ray mapping (EDXM) and the corresponding images of the membrane cross section were taken at an acceleration voltage of 20 kV and an acceleration current of 10 μA. The X-ray diffractometer (XRD) patterns were recorded at room temperature under ambient conditions with Bruker D8 ADVANCE X-ray diffractometer with Cu Ka radiation at 40 kV and 40 mA. FT-IR spectra were obtained by using Bruker TENSOR27 impact spectrometer. Nuclear magnetic resonance (NMR) spectra were obtained at ambient temperature using a Bruker 400 MHz instrument (NMR Switzerland Bruker 400MHz AVANCE III). The signals are presented relative to TMS as 0 ppm, and DMSO was used for solvent. Solid-state NMR experiments were performed on a Bruker WB Avance II 400 MHz spectrometer. The 13C CP/MAS NMR spectra were recorded with a 4-mm double-resonance MAS probe and with a sample spinning rate of 10.0 kHz; a contact time of 2 ms (ramp 100) and pulse delay of 3 s were applied. Thermogravimetric analyses (TGA) were carried out using a Mettler Toledo TGA/STDA 851e. Samples (10 mg) which had been solvent exchanged with dry methanol and degassed at 150 °C, placed in 70 μL alumina pans were heated in a N2 gas flow (20 ml/min) from 20 to 800 ºC at a heating rate of 5 ºC/min. BET surface area measurements were collected at 77 K using nitrogen on an

automatic volumetric adsorption apparatus (Micrometrics ASAP 2020). Prior to measurements, the samples were heated at 150 °C for 6 h under vacuum. After adsorption, the samples were regenerated by degassing under vacuum at room temperature for a few hours. The pore size distribution was estimated from the 77 K N_2 isotherms using a Slit Pore Geometry (original H-K) model fit.

Measurement of the nanofiltration performance: The separation performance of IISERP-COF1 and IISERP-COOH-COF1 membranes was tested using a home-built membrane cross-flow filtration apparatus at room temperature with aqueous solutions at a pressure difference of 2 bar (Fig. S11). One end of the membrane was sealed with silicone, and the other open end was assembled in the module. The effective area of the membrane is approximately 22.6 cm^2. The water flux and rejection of metal ions and methyl blue were tested using deionized (DI) water, 2000 ppm aqueous salt solutions (i.e., NaCl, Na_2SO_4 $FeCl_3$, $MgCl_2$, and $MgSO_4$). To attain stable separation performance, the filtration system was cycled a period of time until reaching a steady state.

Rejection was calculated from conductivity of feed and filtrate solutions using Eq. (1), where C_f and C_p represent the ion concentrations in the feed and the permeate, respectively. The concentrations of salt in the feed and permeate were analysed by a conductivity meter (DDS-11A, INESA Scientific Instrument Co., Ltd., China).

$$R = (1-C_p/C_f) \times 100\% \quad (1)$$

Water Flux (F) is determined by Eq. (2), where Δw is weight of permeate during filtration time Δt, A is the membrane area, ρ is density of permeate and we here consider it to be 1 $g \cdot ml^{-1}$ because of its low salt concentration.

$$F = \Delta w/(\rho A \Delta t) \quad (2)$$

Here, permeance is defined as flux per unit applied pressure, see in Eq (3), where ΔP is the applied trans-membrane pressure for filtration experiment, here it is 2 bar.

$$\text{Permeance}=F/\Delta P \quad (3)$$

The water flux and ion rejection were obtained from the averaged value of three data points.

Stability tests of the IISERP-COOH-COF1 membranes: The long-term stability performance of the IISERP-COOH-COF1 membranes were carried out in the same filtration cell and evaluated by a 168 h (7 days) continuous filtration test at 2 bar using 2000 ppm Na_2SO_4 solutions. To investigate the chemical stability of IISERP-COOH-COF1 membranes in harsh conditions, namely the membrane coupons were soaked in 1.0 M HCl (pH = 1) and 1.0 M NaOH (pH = 13) aqueous solution for 168 h (7 days), respectively. After that, permeance and rejection of thus-treated membranes were measured and compared with those of the membrane without treatment.

Simulation Details:

To provide microscopic insights into the nanofiltration through the COF membranes, molecular simulations were performed. Fig. S12a shows the atomic structure of IISERP-COF1 constructed from the experimentally determined coordinates [2] with lattice constants $a = b$ =1.978 nm, c = 0.378 nm, $\alpha = \beta$ = 90°, and γ = 120°. The atomic model of IISERP-COOH-COF1 as illustrated in Fig. S12b was built by adding the functional groups to IISERP-COF1. Three layers of each COF were constructed with a thickness of approximately 1.13 nm along the *z*-axis (2 × 2 × 3) and used as the membrane in the simulation of nanofiltration. As illustrated in Fig. S12c, a typical simulation system contained two chambers (a NaCl solution on the left and pure water on the right), which were separated by the COF membrane along the *z*-axis. Additionally, two graphene sheets acting as pistons were added into the feed and permeate chambers and they could self-adjust their positions during the simulation under hydraulic pressures P_{feed} and P_{permeate}, respectively. The periodic boundary conditions were applied in *x*- and *y*-axis, and a vacuum layer was added on each side of the simulation system to diminish the effect of periodic images. The interactions of the COF atoms were described by the Lennard-Jones (LJ) and electrostatic interactions. The LJ parameters were adopted from the universal force field (UFF) [10]. The atomic charges

were estimated using the Density-Derived Electrostatic and Chemical (DDEC) method [11], which was based on density functional theory calculations using the Vienna Ab Initio Simulation Package (VASP) [12]. Water, Na^+ and Cl^- ions were represented by the TIP3P model [13] and the Amber force field [14], respectively. The carbon atoms in graphene sheets were described with the LJ parameters as used for carbon nanotubes [15].

The system was first subjected to energy minimization using the steepest descent method; then, velocities were generated according to the Maxwell−Boltzmann distribution, and finally MD simulation was performed at 300 K in a canonical ensemble with P_{feed} = 601 bar and $P_{permeate}$ = 1 bar. It is noteworthy that the pressure difference applied was higher than the common value in nanofiltration. This is common in MD simulations in order to reduce thermal noise and enhance signal/noise ratio within a nanosecond simulation timescale. For example, a high pressure (up to 6000 bar) was used to simulate water permeation [16-17]. During the simulation, the COF membrane was assumed to be rigid. The equations of motion were integrated by the leapfrog algorithm with a time step of 2 fs. A cutoff of 14 Å was used to calculate the LJ interactions and the particle-mesh Ewald method was used to evaluate the electrostatic interactions with a grid spacing of 1.2 Å. The temperature was controlled by a velocity-rescaling thermostat with a relaxation time of 0.1 ps. The MD simulation was performed for 20 ns using GROMACS v.5.1.2 [18].

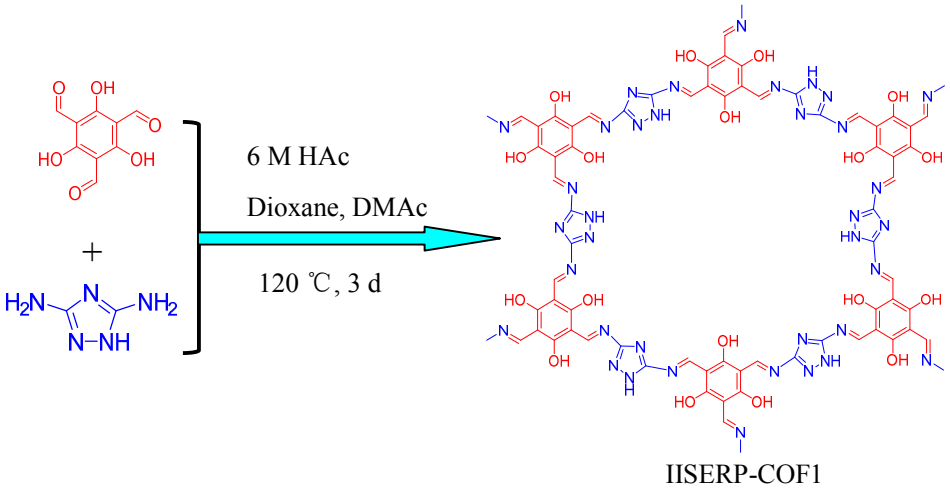

Fig. S1. Scheme of the reaction procedure for the synthesis of the IISERP-COF1.

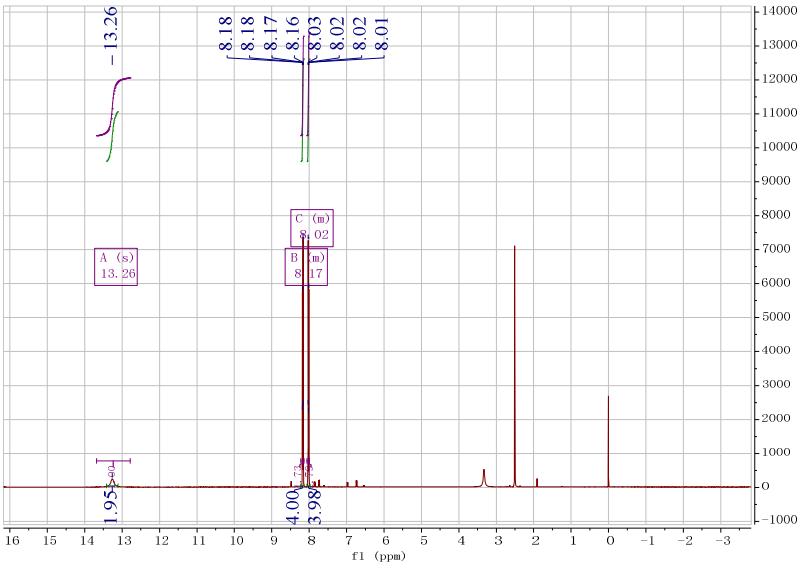

Fig. S2. ^{1}H NMR spectrum for synthesized azobenzene-4, 4'-dicarboxylic acid (500 MHz, DMSO-d6, 298K, TMS): 8.02 ppm, 8.17 ppm (8H, m, ArH), 13.26 ppm (2H, s, -COOH).

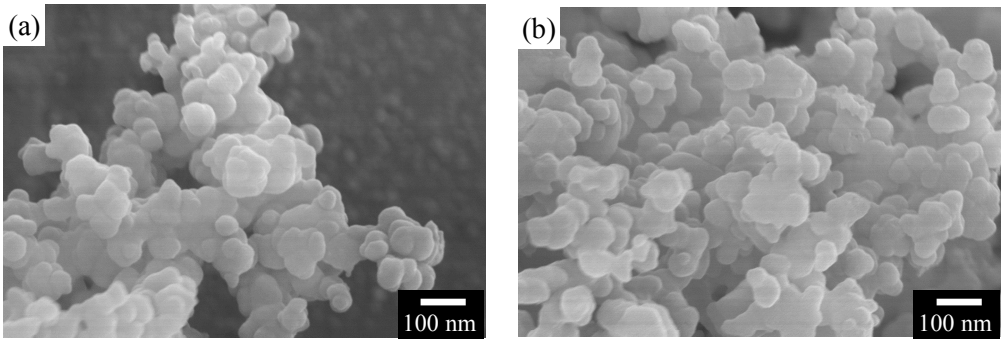

Fig. S3. Typical FESEM image of the IISERP-COF1 (a), and IISERP-COOH-COF1 crystals (b).

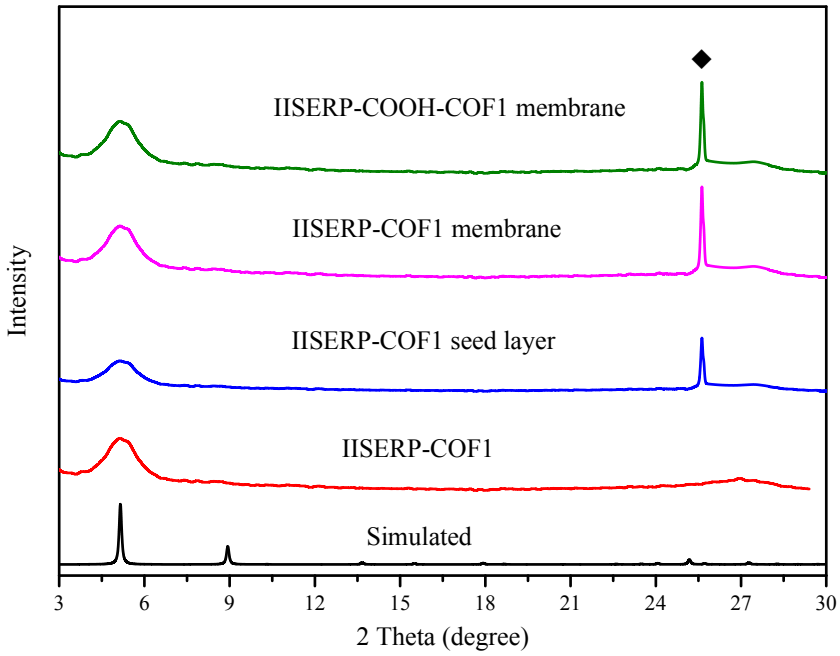

Fig. S4. Typical XRD patterns of the simulated IISERP-COF1, IISERP-COF1 crystals, IISERP-COF1 membrane and IISERP-COOH-COF1 membrane. (◆) Al_2O_3 support. (Not marked) IISERP-COF1 crystals.

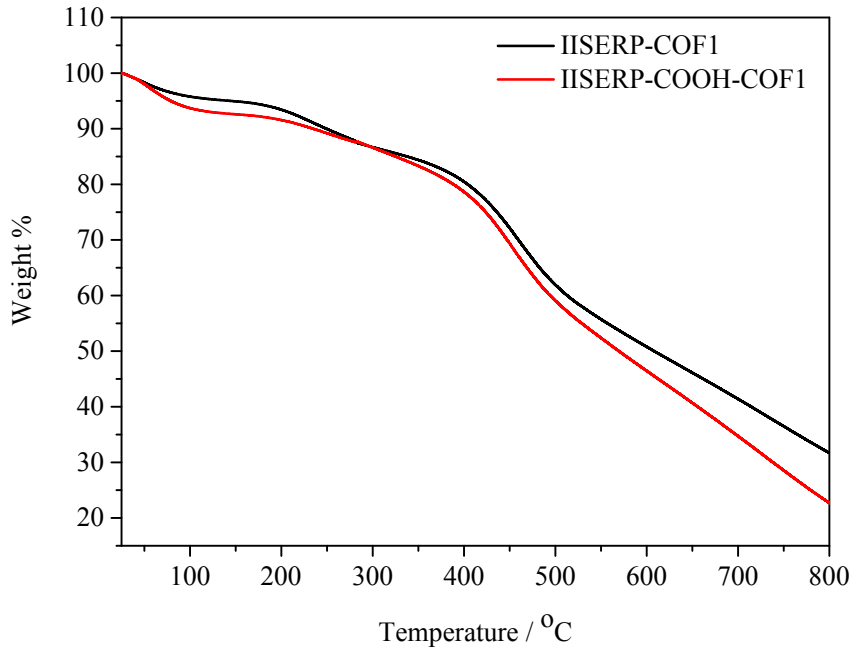

Fig. S5. TGA curve of IISERP-COF1 and IISERP-COOH-COF1 at a heating rate of 10 ^{o}C min^{-1} to 800 ^{o}C with a N_2 flow rate at 30 mL·min^{-1}.

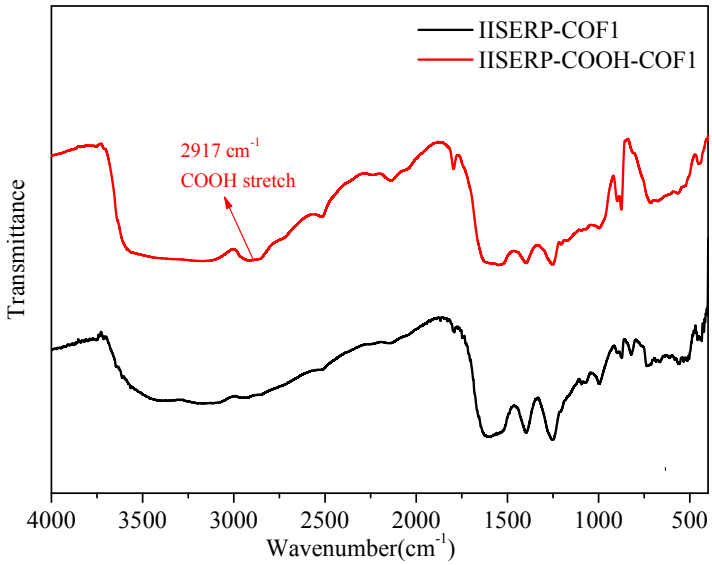

Fig. S6. FT-IR spectrum of IISERP-COF1 and IISERP-COOH-COF1.

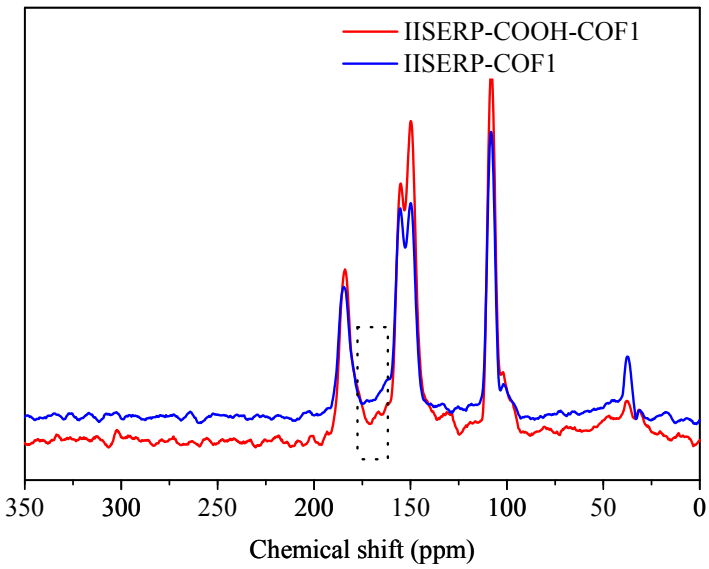

Fig. S7. Solid-state ^{13}C NMR spectra of IISERP-COF1 and IISERP-COOH-COF1.

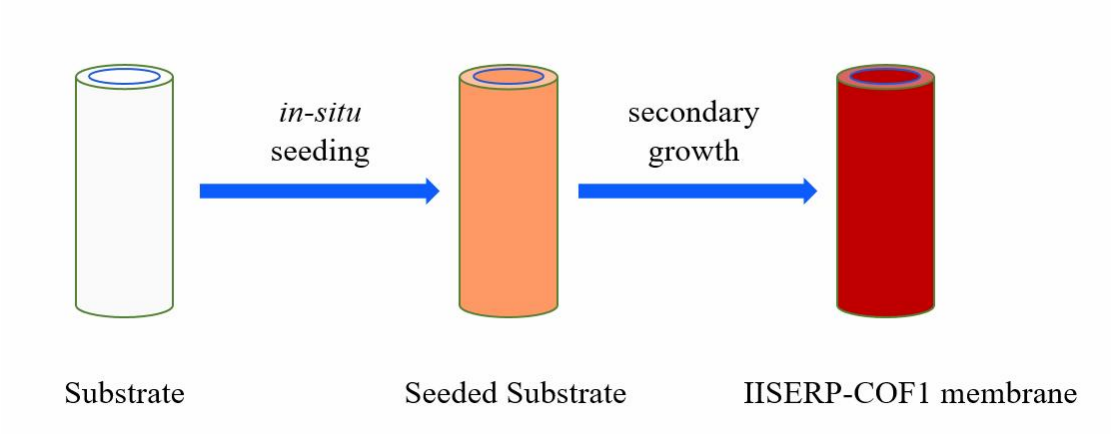

Fig. S8. Illustration of the fabrication process of tubular IISERP-COF1 membranes by secondary growth method.

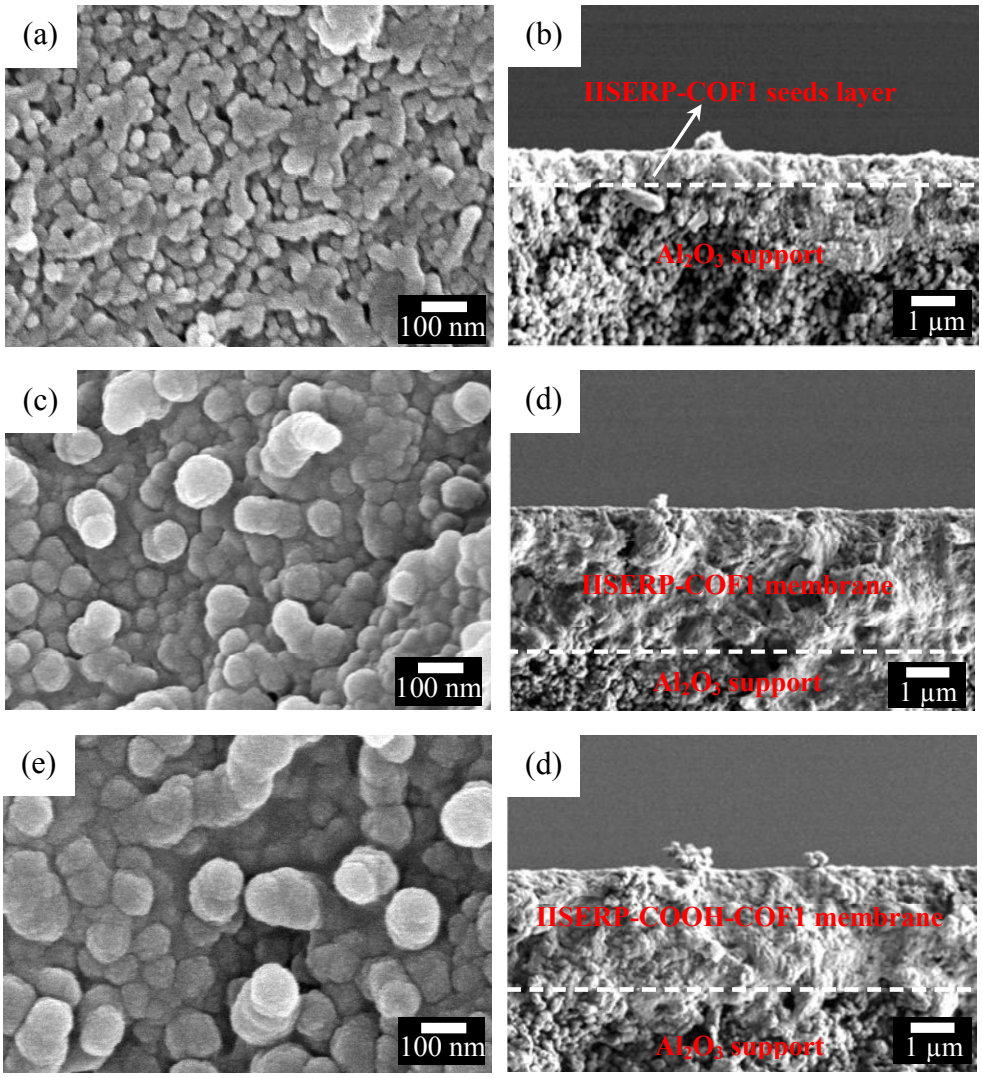

Fig. S9. Top view of (a) and cross-section (b) FESEM images of the IISERP-COF1 seed layer prepared on the alumina tube; top view of (c) and cross-section (d) FESEM images of the IISERP-COF1 membrane prepared on the alumina tube; top view of (e) and cross-section (f) FESEM images of the IISERP-COOH-COF1 membrane prepared on the alumina tube.

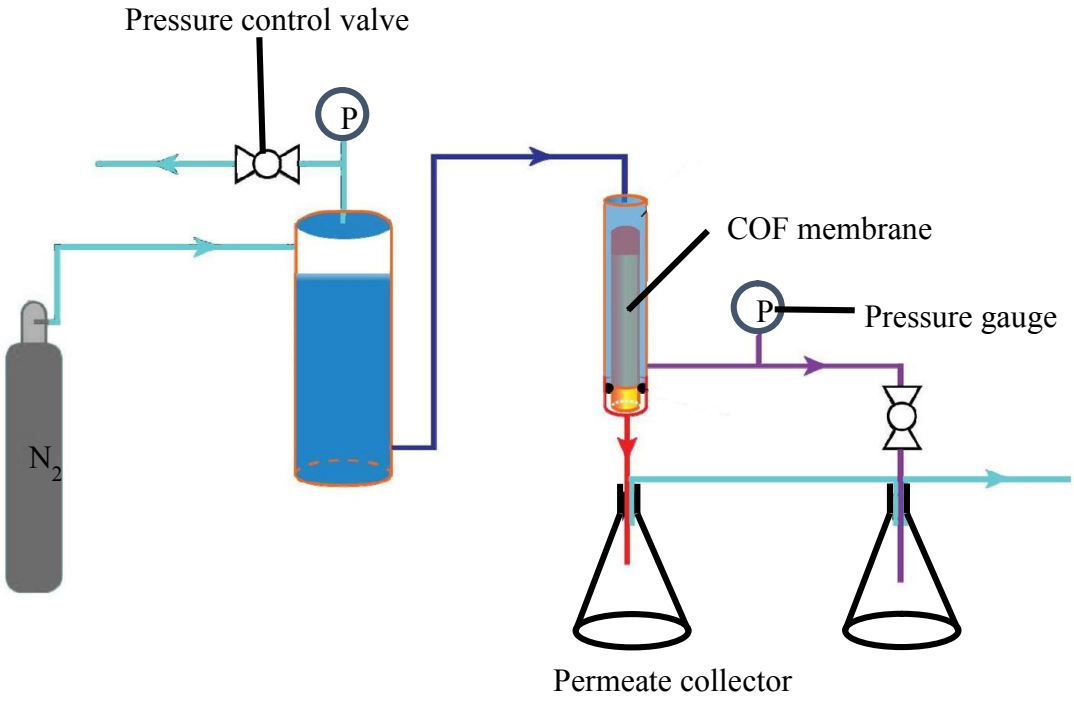

Fig. S10. Schematic diagram of the apparatus for metal ions and methyl blue removal from water.

Molecular weight cut-off (MWCO) of the IISERP-COOH-COF1 membrane was determined with the MW of a test polyethylene glycol (PEG) molecule that has a rejection of 90% (K. Y. Wang, T. Matsuura, T.-S. Chung, and W. F. Guo, J. Membr. Sci., 2004, 240, 67-79; Q. Yang, T.-S. Chung, and Y. Santoso, J. Membr. Sci., 2007, 290, 153-163). The MWCO was measured by using several PEG molecules (with MWs in the range of 300 ~ 3000 Da) at 2000 ppm concentration at room temperature under the pressure of 2 bar. As shown in **Fig. S11**, when the IISERP-COOH-COF1 membranes reach 90% rejection, an MW of about 750 Da is obtained, which is then taken as the MWCO of the IISERP-COOH-COF1 membrane.

The pore size of the membrane can be estimated by the Stokes radiu. The Stokes radiu of the solute was calculated based on average molecular weights as follow equation:

$$r = 16.73 \times 10^{-12} \times M_w^{0.557}$$

Where r is the Stokes radius (m) and M*w* the molecular weight (1 Da = 1 g/mol) (K. Y. Wang, T. Matsuura, T.-S. Chung, and W. F. Guo, J. Membr. Sci., 2004, 240, 67-79; Q. Yang, T.-S. Chung, and Y. Santoso, J. Membr. Sci., 2007, 290, 153-163; M. Meireles, A. Bessieres, I. Rogissart, P. Aimar and V. Sanchez, J. Membr. Sci., 1995, 103, 105-115).

As mention above, the MWCO value of the IISERP-COOH-COF1 membranes is about 750 Da, thus the pore size of the membrane is calculated as about 0.66 nm, which is in good agreement with the pore size obtained by the BET characterization.

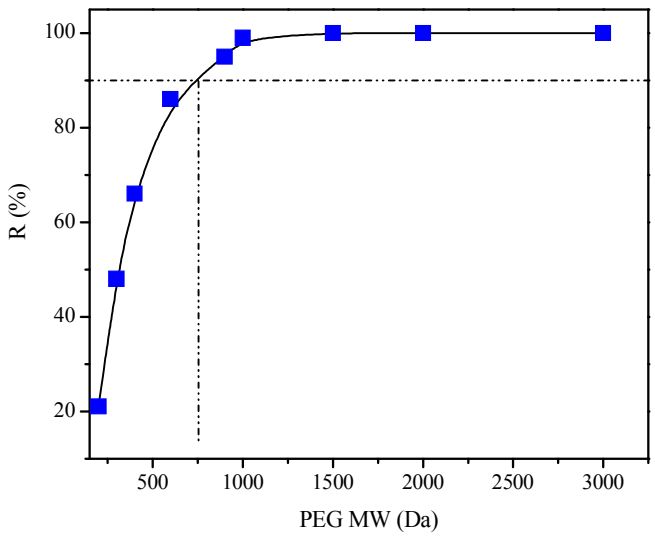

Fig. S11. PEG rejection by IISERP-COOH-COF1 membrane as a function of dye Molecular Weight at 2 bar. The MWCO is determined from the dashed lines shown (1 Da=1 g/mol).

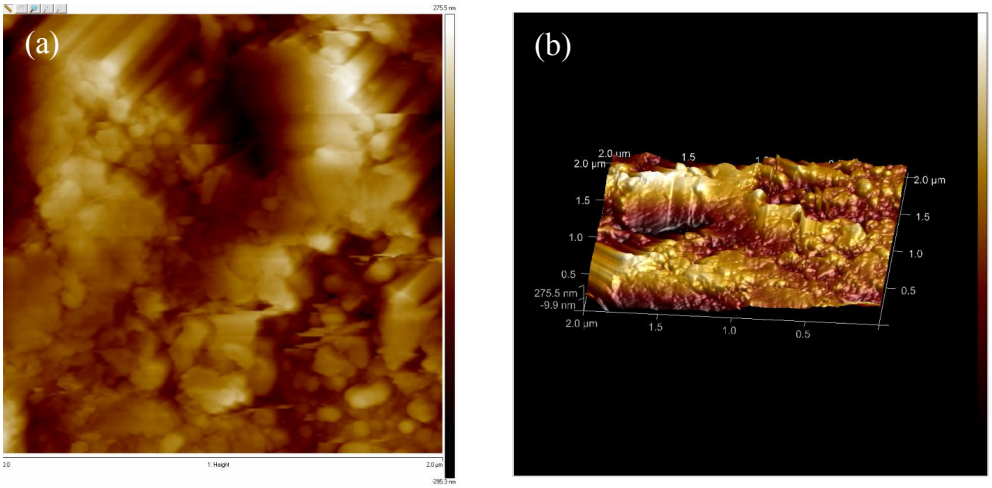

Fig. S12. AFM image of the IISEPR-COOH-COF1 membrane. (a) 2D (2 × 2 μm^2), (b) 3D (2 × 2 × 2 μm^3).

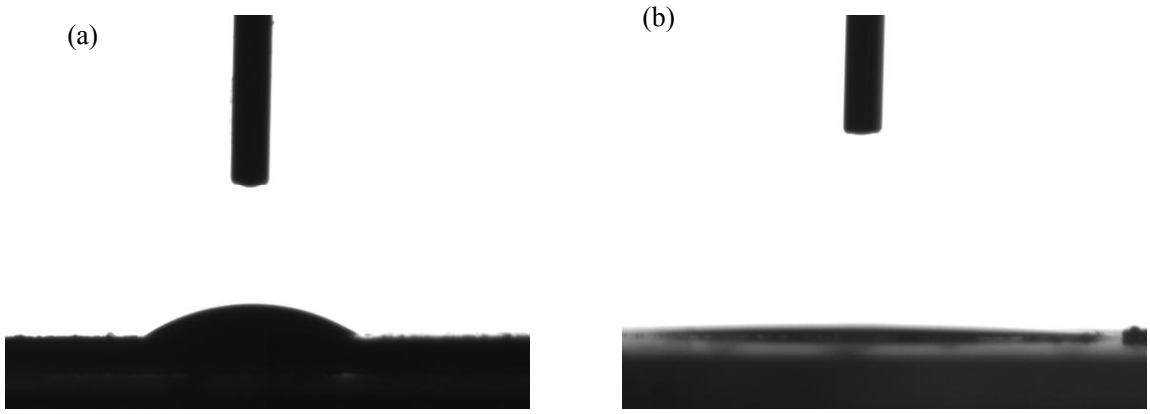

Fig. S13. Water contact angle (CA) measurement of the IISEPR-COF1 membrane (a) and IISEPR-COOH-COF1 membrane (b).

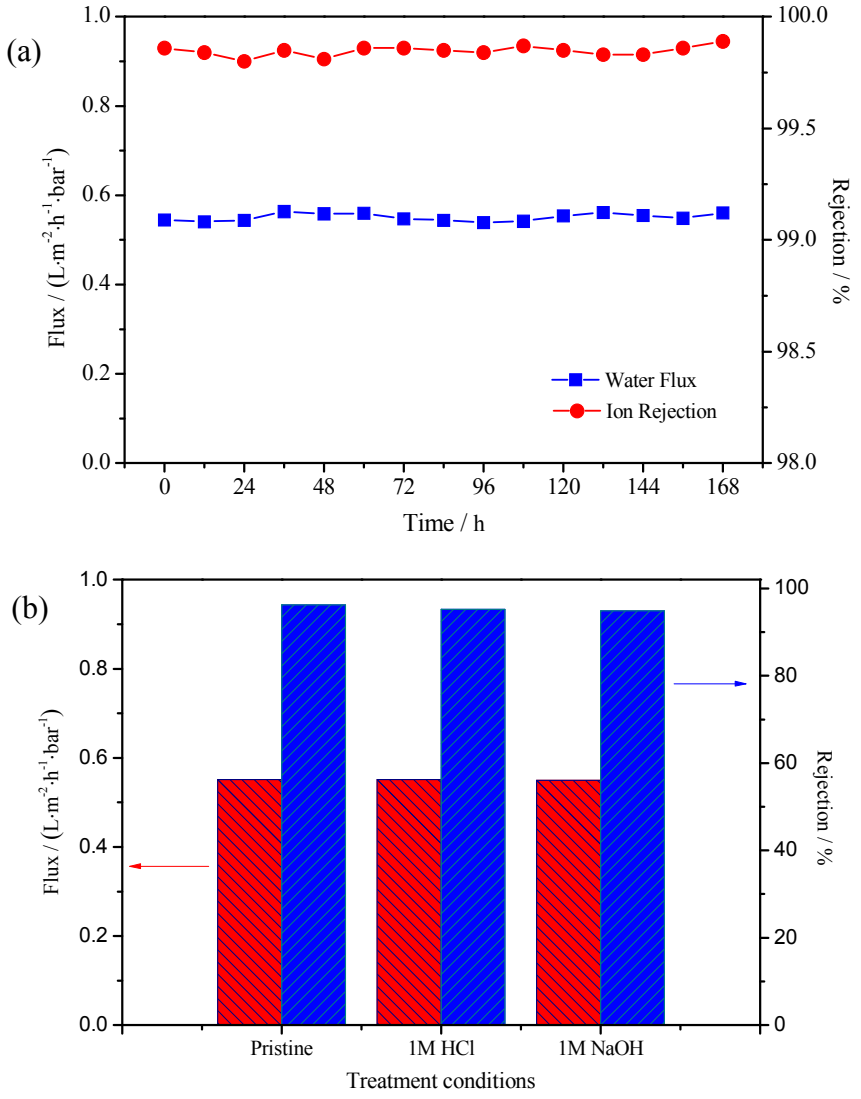

Fig. S14. Stability of the IISERP-COOH-COF1 membranes. (a) Long-term stability of IISERP-COOH-COF1 membranes towards 2000 ppm aqueous Na_2SO_4 solutions. (b) Chemical stability: separation performance versus harsh treatment of the IISERP-COOH-COF1 membranes.

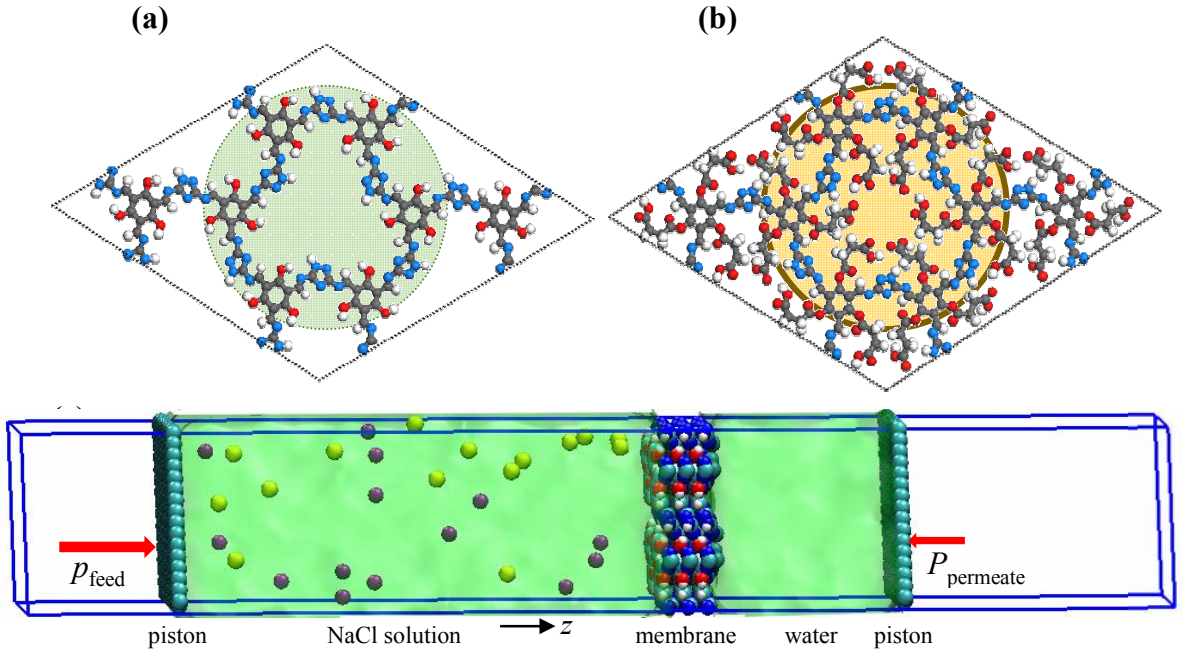

Fig. S15. Atomic structures of (a) IISERP-COF1 and (b) IISERP-COOH-COF1. (c) A simulation system for nanofiltration.

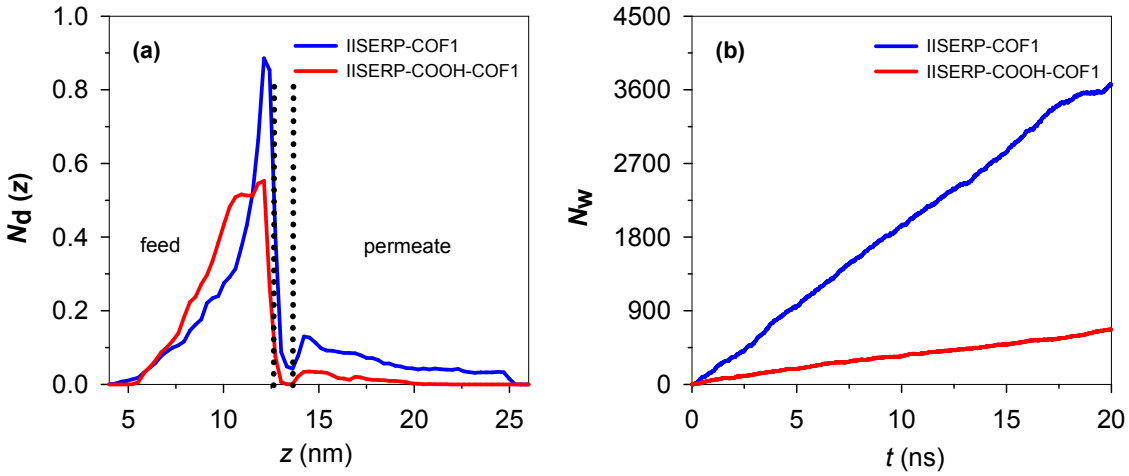

Fig. S16. (a) Number distributions of ions (b) water flows through IISERP-COF1 and IISERP-COOH-COF1 membranes. The membrane is denoted by the dotted lines.

Table S1

Table S1. Permeating flux and rejection of IISERP-COF1 and Carboxylated-IISERP-COOH-COF1 membranes. The concentration of ionic aqueous solution is 2000 ppm. The applied pressure is 2 bar.

Membrane	Na_2SO_4		$MgSO_4$		$FeCl_3$		$MgCl_2$		NaCl	
	F*	R*	F	R	F	R	F	R	F	R
IISERP-COF1	0.63	73.2	0.59	76.5	0.57	89.8	0.60	64.6	0.65	56.4
Carboxylated-IISERP-COF1	0.55	96.3	0.51	97.2	0.48	99.6	0.52	90.6	0.56	82.9

Note: * F represents water flux ($L \cdot m^{-2} \cdot h^{-1} \cdot bar^{-1}$), R represents ion rejection (%)

Table S2

Table S2. Kinetic Diameters of Water, Hydrated Metal Ions and Dyes

Hydrated Metal Ions/Dyes	Diameters* / Å
Water	2.8
Na^{+}	7.16
Mg^{2+}	8.56
Fe^{3+}	9.14
Cl^{-}	6.64
SO_4^{2-}	10

Note: * Diameters was quoted from references [19-21]

Table S3

Table S3. Nanofiltration performance of polycrystalline MOF and COF membranes.

Membranes	Substrate	Classification [a]	Feed composition and pressure difference	Flux ($Lm^{-2}h^{-1}bar^{-1}$)	R / %	Stability [b]	Ref.
UiO-66	Al_2O_3 hollow fiber	Pure MOF	0.2 % seawater, 10 bar	0.14	98	No stable in alkaline	22
UiO-66-NH_2	Al_2O_3 tube	Pure MOF	3.5 % seawater, 1 bar	1.5	>99.7	No stable in alkaline	23
PSDH UiO-66-$(OH)_2$	Al_2O_3 hollow fiber	Pure MOF	0.2 % Na_2SO_4, 3 bar	0.21	45	No stable in alkaline	24
COF-LZU1	Al_2O_3 tube	Pure MOF	0.2 % Na_2SO_4 5 bar	0.94	4.5	stable	25
PES+polyimine COF	PES support	Hybrid	400 mg/L NaCl, 5 bar	NA	~10	stable	26
TpPa-1	PVDF	Pure COF	50 μmol/L dye solutions Congo red, 2.5 bar	25	98.7%	stable	27
TpPa-AAO	AAO	Pure COF	0.5 g L^{-1}, BSA solution	1263	88.6	stable	28
GO–CTF5	polycarbonate support	Hybrid	100 ppm of dye solution	226.3	>90%	stable	29
TpTGCl@CNFs	PAN	Hybrid	0.1 wt% Na_2SO_4 solution, 6 bar	42.8	96.8	No stable in acidic or alkaline	30
NF-270	None	Polymer	1000 mg L^{-1} Na_2SO_4 , 6bar	10.3	96.1	No stable in acidic or alkaline	31
SOD zeolite	Al_2O_3 disk	Pure zeolite	North seawater, 22 bar	0.24	>99.99	No stable in Acid	32
MFI zeolite	Al_2O_3 disk	Pure zeolite	0.10 M NaCl, 20.7 bar	0.112	76.7	No stable in Acid	33
MFI zeolite	Al_2O_3 disk	Pure zeolite	0.10 M NaCl, 21 bar	0.162	21.6	No stable in Acid	34
Polyarylate	XP84	Polymer	100 ppm of methanol solution	0.6	>99	No stable in harsh conditions	35
p-CMP-OOC7	PAN	Polymer	100 ppm of methanol solution	1.10	>99	No stable in harsh conditions	36
IISERP-COF1	Al_2O_3 tube	3200	0.2 % Na_2SO_4 2 bar	0.63	73.1	stable	This work
Carboxylated-IISERP-COF1	Al_2O_3 tube	3200	0.2 % Na_2SO_4, 2 bar	0.55	96.3	stable	This work

[a] the membrane can be divided into three categories, namely pure MOF membrane, pure COF membrane, pure polymer membrane and hybrid membrane.

[b] Stability means that the membrane should be stable in harsh conditions (Under acidic or alkaline conditions); most MOF membrane cannot be stable in harsh conditions. Pure polymer membrane ages under acidic conditions, causing performance degradation. As for COF membrane, most of them are stable in harsh conditions.

References in Supporting Information:

1. J. H. Chong, M. Sauer, B. O. Patrick and M. J. MacLachlan, *Org. Lett.*, 2003, **5**, 3823-3826.
2. S. Haldar, K. Roy, S. Nandi, D. Chakraborty, D. Puthusseri, Y. Gawli, S. Ogale and R. Vaidhyanathan, *Advanced Energy Materials*, 2018, **8**, 1702170.
3. A. Huang, H. Bux, F. Steinbach and J. Caro, *Angew. Chem. Int. Ed.*, 2010, **49**, 4958-4961.
4. A. Huang, W. Dou and J. r. Caro, *J. Am. Chem. Soc.*, 2010, **132**, 15562-15564.
5. A. Huang, F. Liang, F. Steinbach and J. Caro, *J. Membr. Sci.*, 2010, **350**, 5-9.
6. A. Huang, N. Wang and J. Caro, *J. Membr. Sci.*, 2012, **389**, 272-279.
7. A. Huang, N. Wang and J. Caro, *Microporous Mesoporous Mater.*, 2012, **164**, 294-301.
8. N. Huang, X. Chen, R. Krishna and D. Jiang, *Angew. Chem. Int. Ed.*, 2015, **54**, 2986-2990.
9. Q. Lu, Y. Ma, H. Li, X. Guan, Y. Yusran, M. Xue, Q. Fang, Y. Yan, S. Qiu and V. Valtchev, *Angew. Chem. Int. Ed. Engl.*, 2018, **57**, 6042-6048.
10. A. K. Rappe, C. J. Casewit, K. S. Colwell, W. A. Goddard and W. M. Skiff, *J. Am. Chem. Soc.*, 1992, **114**, 10024-10035.
11. T. A. Manz and D. S. Sholl, *J. Chem. Theory. Comput.*, 2010, **6**, 2455-2468.
12. J. Hafner, *J. Comput. Chem.*, 2008, **29**, 2044-2078.
13. W. L. Jorgensen, J. Chandrasekhar, J. D. Madura, R. W. Impey and M. L. Klein, *J. Chem. Phys.*, 1983, **79**, 926-935.
14. W. D. Cornell, P. Cieplak, C. I. Bayly, I. R. Gould, K. M. Merz, D. M. Ferguson, D. C. Spellmeyer, T. Fox, J. W. Caldwell and P. A. Kollman, *J. Am. Chem. Soc.*, 1995, **117**, 5179-5197.
15. G. Hummer, J. C. Rasaiah and J. P. Noworyta, *Nature*, 2001, **414**, 188.
16. D. Cohen-Tanugi and J. C. Grossman, *Nano Lett.*, 2012, **12**, 3602-3608.
17. T. A. Hilder, D. Gordon and S.-H. Chung, *Small*, 2009, **5**, 2183-2190.
18. M. J. Abraham, T. Murtola, R. Schulz, S. Páll, J. C. Smith, B. Hess and E. Lindahl, *SoftwareX*, 2015, **1-2**, 19-25.
19. E. Nightingale Jr, *J. Chem. Phys.*, 1959, **63**, 1381-1387.
20. S. Kandambeth, B. P. Biswal, H. D. Chaudhari, K. C. Rout, S. Kunjattu H, S. Mitra, S. Karak, A. Das, R. Mukherjee and U. K. Kharul, *Adv. Mater.*, 2017, **29**, 1603945.
21. S. Karan, Z. Jiang and A. G. Livingston, *Science*, 2015, **348**, 1347-1351.
22. X. Liu, N. K. Demir, Z. Wu and K. Li, *J. Am. Chem. Soc.*, 2015, **137**, 6999-7002.
23. L. Wan, C. Zhou, K. Xu, B. Feng and A. Huang, *Microporous Mesoporous Mater.*, 2017, **252**, 207-213.
24. X. Wang, L. Zhai, Y. Wang, R. Li, X. Gu, Y. D. Yuan, Y. Qian, Z. Hu and D. Zhao, *ACS Applied Materials & Interfaces*, 2017, DOI: 10.1021/acsami.7b12750.
25. H. Fan, J. Gu, H. Meng, A. Knebel and J. Caro, *Angew. Chem. Int. Ed., 2018, **57(15)**, 4083-4087.*.
26. L. Valentino, M. Matsumoto, W. R. Dichtel and B. J. Mariñas, *Environ. Sci. Technol.*, 2017, **51**, 14352-14359.
27. R. Wang, X. Shi, Z. Zhang, A. Xiao, S.-P. Sun, Z. Cui and Y. Wang, *J. Membr. Sci.*, 2019.
28. X. Shi, A. Xiao, C. Zhang and Y. Wang, *J. Membr. Sci.*, 2019, **576**, 116-122.
29. N. A. Khan, J. Yuan, H. Wu, L. Cao, R. Zhang, Y.-n. Liu, L. Li, A. U. Rahman, R. Kasher and Z. Jiang, *ACS applied materials & interfaces*, 2019.
30. H. Yang, L. Yang, H. Wang, Z. Xu, Y. Zhao, Y. Luo, N. Nasir, Y. Song, H. Wu and F. Pan, *Nature communications*, 2019, **10**, 2101.
31. Y. Li, E. Wong, Z. Mai and B. Van der Bruggen, *J. Membr. Sci.*, 2019, **592**, 117396-117406.
32. S, Khajavi.; J, Jansen.. Kapteijn; F, C., *J. Membr. Sci.* 2010, **356**, 52-57.
33. L, Li.; J, Dong.; Nenoff, T . M.; R, Lee., *J. Membr. Sci.* 2004, ***243***, 401-404.
34. L, Li.; J, Dong.; Nenoff, T . M.; R, Lee., *Desalination* 2004, ***170***, 309-316.
35. S. Karan, Z. Jiang, A.G. Livingston, *Science*, 2015, **348**, 1347-1351.
36. B. Liang, H. Wang, X. Shi, B. Shen, X. He, Z.A. Ghazi, N.A. Khan, H. Sin, A.M. Khattak, L. Li, *Nat. Chem.*, 2018, **10**, 961-966.